Glycosylinositolphosphoceramides in Aspergillus fumigatus.

Catherine Simenel, Bernadette Coddeville, Muriel Delepierre, Jean-Paul Latgé, Thierry Fontaine

OXFORD UNIVERSITY PRESS Glycobiology

Glycosylinositolphosphoceramides in Aspergillus fumigatus

Journal:	*Glycobiology*
Manuscript ID:	GLYCO-2007-00125.R1
Manuscript Type:	Regular Manuscripts
Date Submitted by the Author:	n/a
Complete List of Authors:	Simenel, Catherine; Institut Pasteur, Unité de Résonance Magnétique Nucléaire des Biomolécules Coddeville, Bernadette; Université des Sciences et Technologies de Lille, Unité de Glycobiologie Structurale et Fonctionnelle Delepierre, Muriel; Institut Pasteur, Unité de Résonance Magnétique Nucléaire des Biomolécules Latge, Jean-Paul; Institut Pasteur, parasitology Mycology Thierry, Fontaine; Institut Pasteur, Unite des Aspergillus
Key Words:	aspergillus fumigatus, glycosylinositolphosphoceramide, NMR, galactofuranose, glycosphingolipid

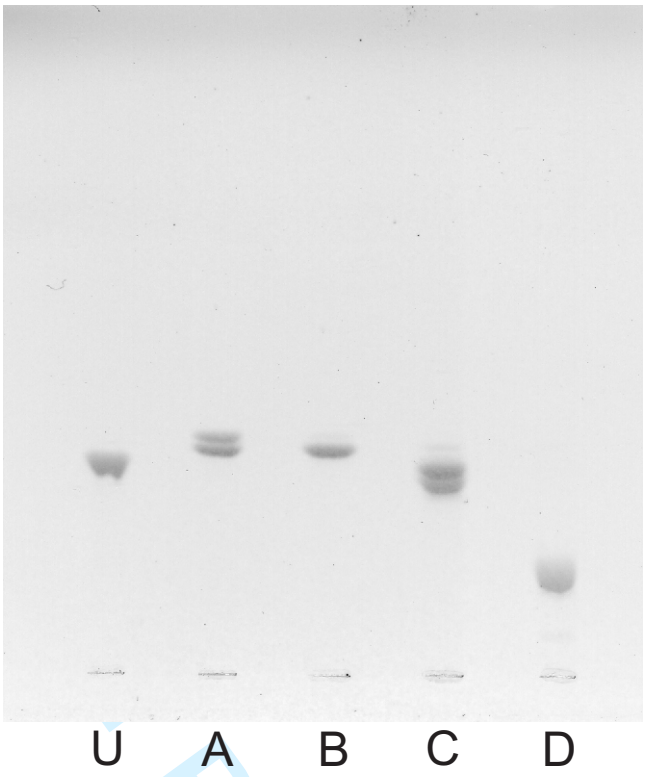

Figure 1

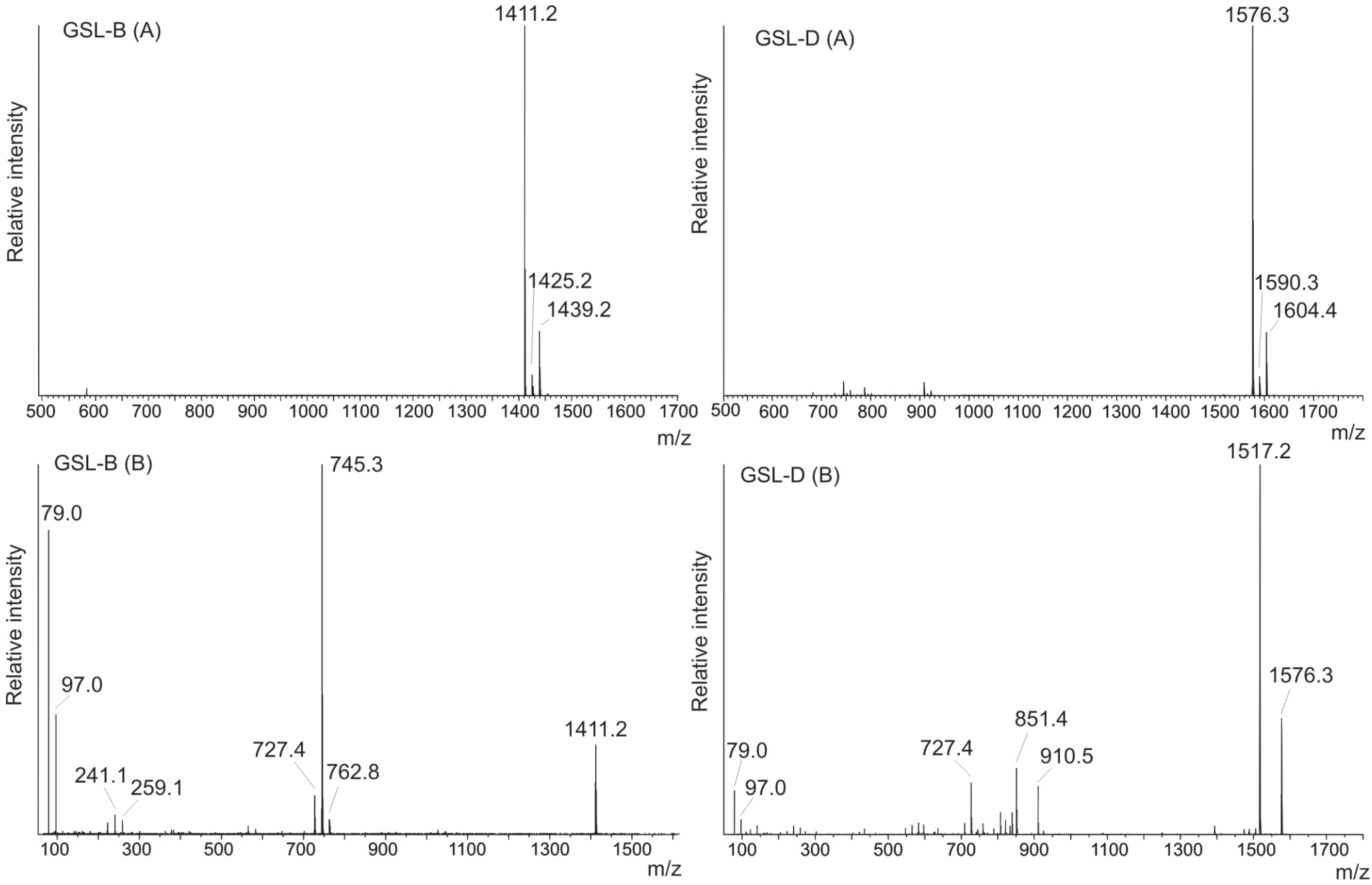
GSL-B (A)
1411.2
1425.2
1439.2
Relative intensity
500 600 700 800 900 1000 1100 1200 1300 1400 1500 1600 1700
m/z
GSL-D (A)
1576.3
1590.3
1604.4
Relative intensity
500 600 700 800 900 1000 1100 1200 1300 1400 1500 1600 1700
m/z
GSL-B (B)
745.3
79.0
97.0
1411.2
727.4
762.8
241.1
259.1
Relative intensity
100 300 500 700 900 1100 1300 1500
m/z
GSL-D (B)
1517.2
1576.3
851.4
79.0
727.4
910.5
97.0
Relative intensity
100 300 500 700 900 1100 1300 1500 1700
m/z

Figure 3

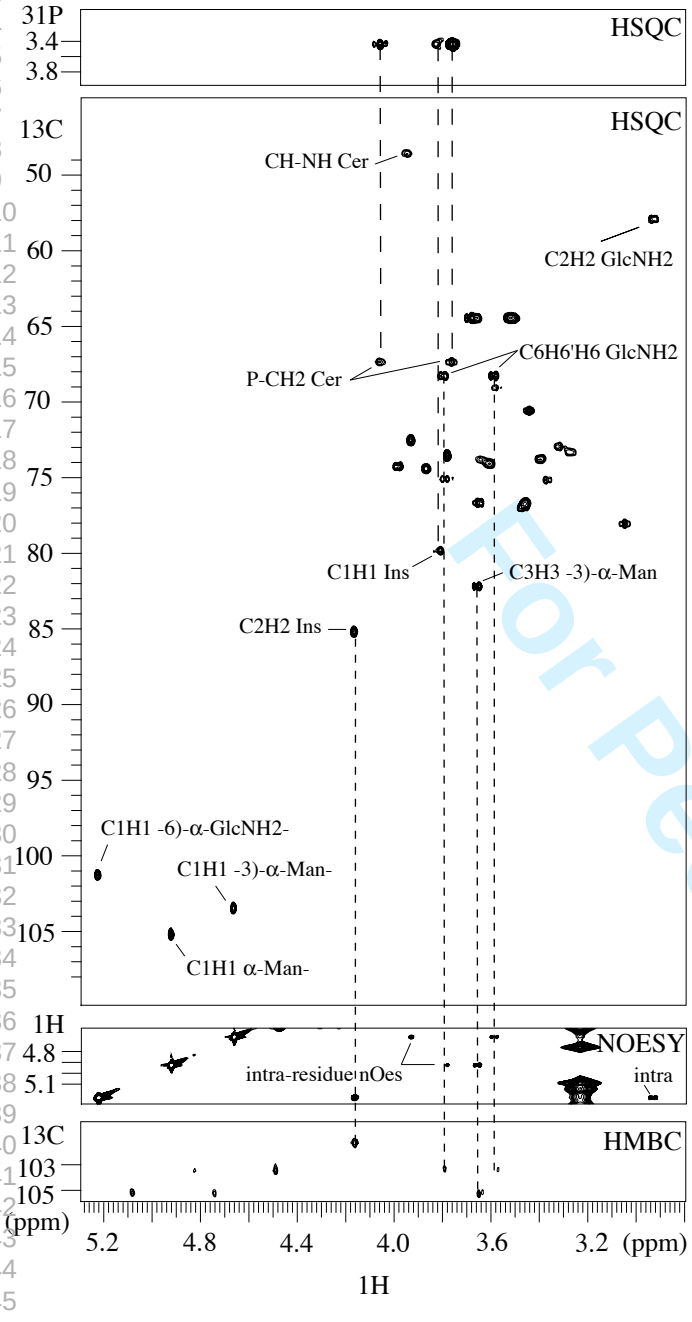

Figure 4

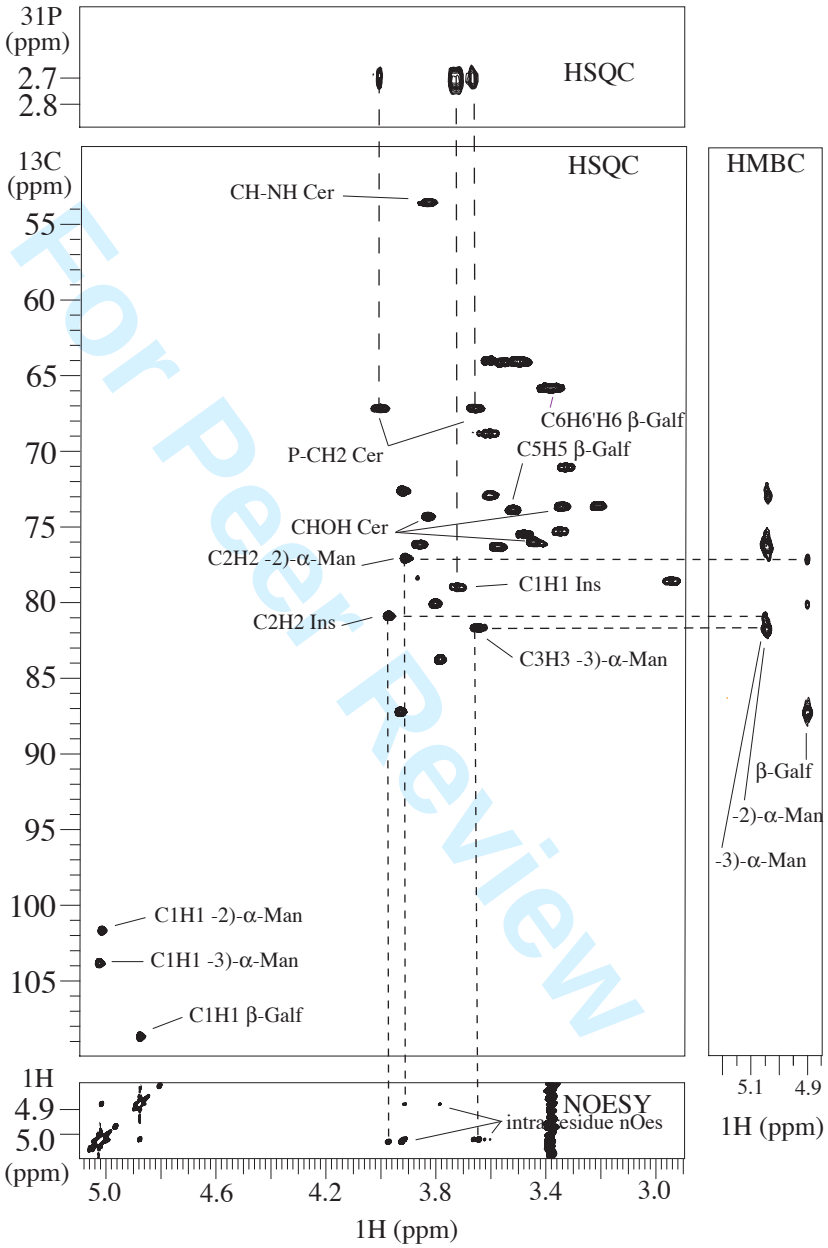

Figure 5

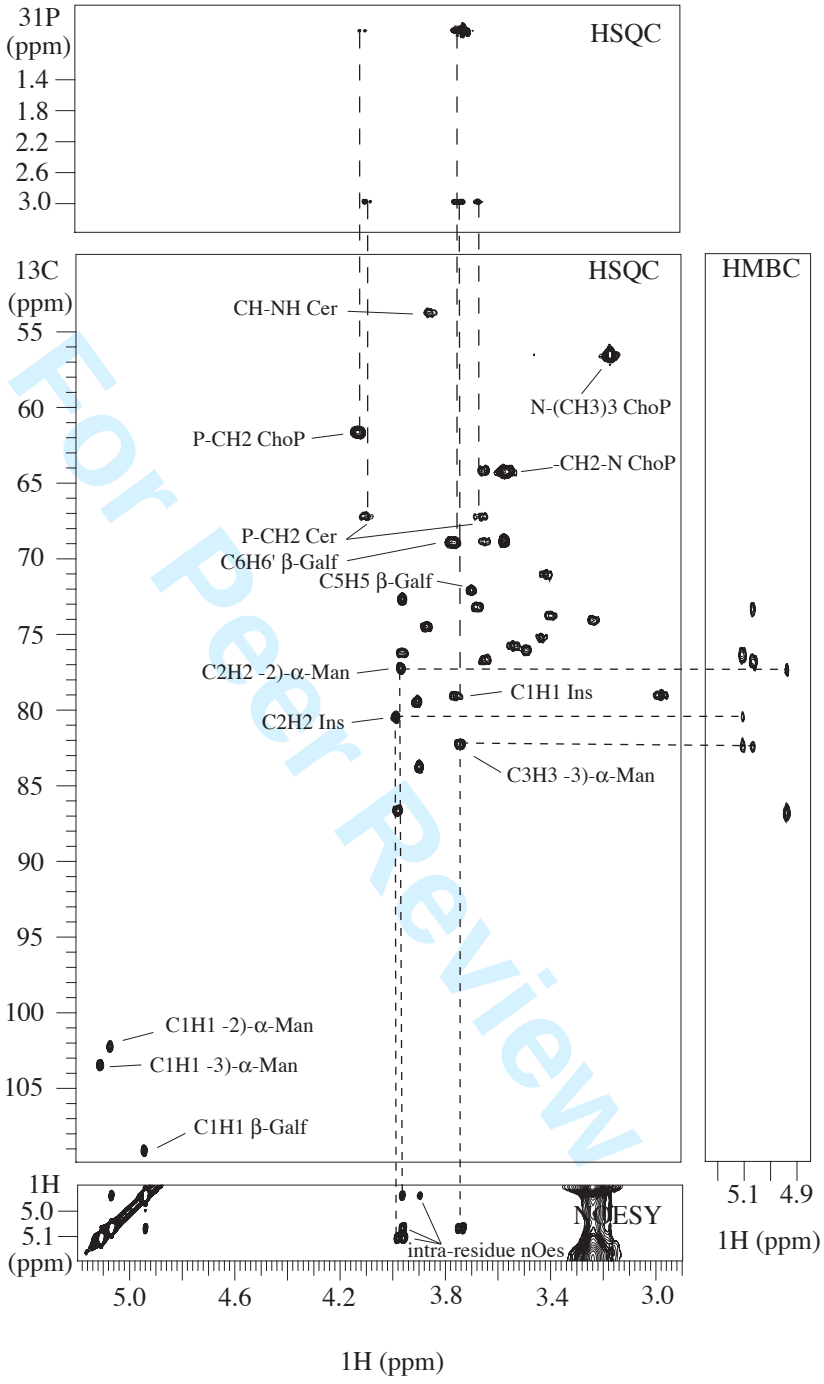

Glycosylinositolphosphoceramides in *Aspergillus fumigatus*

Catherine Simenel[1], Bernadette Coddeville[2], Muriel Delepierre[1], Jean-Paul Latgé[3] and Thierry Fontaine[3]*

Unité de Résonance Magnétique Nucléaire des Biomolécules, CNRS URA 2185 Institut Pasteur, 25 rue du Docteur Roux 75724 Paris cedex 15,

[2]Unité de Glycobiologie Structurale et Fonctionnelle, UMR 8576 CNRS, Université des Sciences et Technologies de Lille, 59655 Villeneuve d'Ascq cedex

Unité des Aspergillus, Institut Pasteur, 25 rue du Docteur Roux 75724 Paris cedex 15.

*corresponding author: tfontain@pasteur.fr

Summary

Fungal glycosylinositolphosphoceramides (GIPCs) are involved in cell growth and fungal-host interactions. In this study, 6 GIPCs from the mycelium of the human pathogen *Aspergillus fumigatus* were purified and characterized using Q-TOF mass spectrometry and ^{1}H, ^{13}C and ^{31}P NMR. All structures have the same inositolphosphoceramide moiety with the presence of a $C_{18:0}$-phytosphingosine conjugated to a 2-hydroxylated saturated fatty acid, (2-hydroxy-lignoceric acid). The carbohydrate moiety defines 2 types of GIPC. The first, a mannosylated zwitterionic glycosphingolipid contains a glucosamine residue linked in α1-2 to an inositol ring that has been described in only two other fungal pathogens. The second type of GIPC presents a α-Manp-(1→3)-α-Manp-(1→2)-IPC common core. A galactofuranose residue is found in 4 GIPC structures, mainly at the terminal position via a β1-2 linkage. Interestingly, this galactofuranose residue could be substituted by a choline-phosphate group, as observed only in the GIPC of *Acremonium sp*., a plant pathogen.

Introduction

Glycosphingolipids (GSLs) are membrane glycolipids found in all eukaryotic cells that are composed of a carbohydrate and a ceramide hydrophobic moiety. In yeast and fungi, three types of GSLs have been identified. The first class is represented by neutral β-glucosyl-ceramide and β-galactosyl-ceramide. This type of GSL plays a crucial role in spore germination, hyphal growth and in the cell cycle (Levery *et al*., 2002; da Silva *et al*., 2004; Barreto-Bergter *et al.*, 2004; Rittershaus *et al*., 2006). The second class of fungal GSLs is composed of a complex neutral moiety and a saturated ceramide, suggesting a different biosynthetic pathway (Maciel *et al*., 2002; Aoki *et al*., 2004b; Barreto-Bergter *et al*., 2004). The third class is composed of glycosylinositolphosphoceramides (GIPCs) which are acidic GSLs containing a phosphodiester linkage between inositol and ceramide. In contrast to cerebrosides, these phosphorylinositol-containing sphingolipids are not present in mammals but have been detected in protozoa, plants, fungi and nematodes. The sphingolipids are essential for fungal growth since the deletion of inositolphosphorylceramide (IPC) synthase that catalyses the transfer of inositol and phosphate to ceramide is lethal in *Saccharomyces* and *Aspergillus* (Nagiec *et al*., 1997; Cheng *et al*., 2001; Hu *et al*, 2007). In filamentous fungi, the ceramide moiety is composed of a phytosphingosine associated with a saturated long chain fatty acid containing 18 to 26 carbon atoms with or without a hydroxyl group in position 2. The carbohydrate moiety is more variable. Three types of GIPCs have been mainly identified based on the monosaccharide and its linkage to the inositol ring: i) α-Man-(1-2)-IPC found in numerous species (Barr *et al*., 1984; Levery *et al*., 1998; 2001; Heise *et al*., 2002), ii) α-Man-(1-6)-IPC, found in *Sporothrix schenckii*, (Loureiro y Penha *et al*., 2001; Toledo *et al*., 2001a) iii) α-GlcN-(1-2)-IPC described in *S. schenckii, Acremonium sp*. and *Aspergillus fumigatus* (Toledo *et al*., 2001b; 2007; Aoki *et al.,* 2004a). To these core structures, other monosaccharides such as fucose, xylose, galactose or choline-phosphate

could be associated (Jennemann *et al*., 1999; Heise *et al.,* 2002; Arigi *et al*., 2007; Gutierrez *et al.,* 2007). The presence of an α-Man-(1-4)-IPC sequence has been only reported in Basidiomycetes, outside the 3 families described suggesting a high level of complexity in the structure of the fungal sphingolipids (Jennemann *et al*., 2001).

A. fumigatus is a saprophytic, filamentous fungus found in most environments where it plays an important role in the recycling of organic materials. *A. fumigatus* is also an opportunistic pathogen responsible for severe pulmonary diseases, particularly in immunocompromised patients (Latgé, 1999). Man_2-IPC and five other GIPC structures containing additional mannose, galactofuranose, glucosamine or N-acetylglucosamine residues have been previously identified in *A. fumigatus* (Levery *et al*, 2001; Toledo *et al*., 2007). This fungus also produces a lipogalactomannan linked to the cellular membrane through a GlcN-IPC (Costachel *et al*., 2005). As an effort to identify cell surface glycans and antigens, four new structures of GIPC were isolated from membrane preparations of *A. fumigatus* mycelium and chemically characterized using mass spectrometry and NMR analysis.

Results

The crude membrane preparation of *A. fumigatus* mycelium was treated with chloroform/methanol/water, then with a butanol/water partition to recover a glycolipid preparation. Two liquid chromatographic steps on a DEAE-Sephadex column and Silica 60 column were used to separate 5 glycosphingolipid fractions (Fig. 1). The total amount of GSLs represented around 0.02 % +/- 0.005 of the total mycelium dry weight. DEAE anion exchange chromatography yielded an unbound glycosphingolipid (GSL-U) and negatively charged GSLs. Similar amounts of unbound and bound fractions were purified from a 15-L fermentor in Sabouraud medium of *A. fumigatus.* Silica gel column chromatography was used to purify the unbound GSL-U and 4 fractions of negatively charged GSLs (GSL-A, GSL-B,

GSL-C, GSL-D) (Fig. 1). The GSL-A and GSL-C fractions contain two molecules. Only one spot was detected in fractions B and D.

Composition analysis obtained by GLC and GLC-MS revealed the presence of $C_{18:0}$-phytosphingosine and a 2-monohydroxylated $C_{24:0}$ fatty acid in all GSL fractions. Minor fatty acids such as 2OH-$C_{25:0}$ and 2OH-$C_{26:0}$ were observed in low amounts (data not shown). Mannose and *myo*-inositol were identified in all GSL fractions, whereas glucosamine was detected only in the GSL-U fraction and galactose only in negatively-charged GSL fractions (GSL-A to D) (Table I).

GSL fractions have been analysed by Q-TOF mass spectrometry to identify the molecular weight of isolated glycosphingolipids; pseudomolecular negative ions m/z are presented in Table 1 and Fig. 2. The pseudomolecular ion at m/z = 1410 obtained with GSL-U fraction corresponded to a glycosphingolipid containing 2 hexose residues and 1 hexosamine associated with an inositolphosphoceramide (IPC) whereas the ceramide was composed of a $C_{18:0}$-phytosphingosine associated with a 2-hydroxylated $C_{24:0}$ fatty acid (Costachel *et al*., 2005). The presence of minor ions that differ by a mass of 14 or 28 reflected the variability in size of fatty acids. Pseudomolecular ions at m/z = 1249, 1411, 1573, obtained with GSL-A, B, C fractions were compatible with a similar IPC with the presence of 2, 3 or 4 hexose residues. A fragmentation pseudomolecular ion at m/z = 1411 produced one main ion at m/z = 745 [Hex_3-inositol-phosphate]$^-$, ions at m/z = 241 and 259 corresponding to inositol-phosphate and ions at m/z = 79 and 97 corresponding to free phosphate (Fig. 2) (Costachel *et al*., 2005). Fragmentation of pseudomolecular ions at m/z = 1249, 1411, 1573 gave similar patterns of fragmentation with the loss of 666 corresponding to the ceramide moiety (data not shown), characterizing a GIPC and indicating the presence of 2, 3 and 4 hexose residues linked to IPC. In contrast, the fragmentation of a pseudomolecular ion at m/z = 1576 in the GSL-D fraction did not produce similar patterns of daughter ions, indicating structural modifications (Fig. 2).

The composition of this GSL-D fraction indicated the presence of the same IPC structure with mannose residues. Indeed, a pseudomolecular mass at m/z = 1576 did not correspond to a classical mannosylated IPC, but instead, the presence of a choline-phosphate linked to a Hex_3-IPC. Daughter fragments at m/z 1517 $[CH_2\text{-}CH_2\text{-}P\text{-}Hex_3\text{-}IPC]^-$, 910 $[(CH_3)_3N\text{-}CH_2\text{-}CH_2\text{-}P\text{-}Hex_3\text{-inositol-}P]^-$, 851 $[CH_2\text{-}CH_2\text{-}P\text{-}Hex_3\text{-inositol-}P]^-$ were in agreement with the presence of a choline-phosphate substituent. Moreover, GLC-MS analysis of the sugar-phosphate following methanolysis and trimethylsilylation of the GSL-D fraction permitted the identification of a monosaccharide-6-phosphate with the same retention time as the galactose-6-phosphate obtained from the lipophosphoglycan of *Leishmania donovani* (data not shown). These data suggest the presence of phosphocholine linked to the C-6 of a galactose residue in the GSL-D fraction.

Linkages of monosaccharides were analysed after methylation (Table II). Methylation of the GSL-U fraction revealed the presence of 3 methyl ethers corresponding to a terminal mannose, a mannose substituted in position 3, and a glucosamine substituted in position 6. In agreement with Q-TOF mass spectra and to GSL described in fungal species (Toledo *et al*., 2001b; 2007; Aoki *et al*., 2004a), these data suggest the following sequence: Man1-3-Man1-6GlcN. In the GSL-A fraction, the presence of 2 terminal monosaccharides, a mannose and a galactofuranose, without a disubstituted monosaccharide confirmed the presence of two GSL structures. GSL-B fraction contained 3 major methyl ethers with a terminal galactofuranose, indicating, in agreement with the Q-TOF mass spectra, a Gal-Man-Man sequence. In the GSL-C fraction, a disubstituted mannose in position 3 and 6 indicated a branched structure with a terminal galactofuranose and/or mannose. In the GSL-D fraction, 2 main methyl ethers corresponding to monosubstituted mannoses have been identified, but no terminal monosaccharide. A stronger acid hydrolysis yielded a 2,3,5-tri-O-methyl hexitol that should correspond to a galactofuranose substituted in position 6 by a phosphate identified after

methanolysis and trimethysilylation. In agreement with the Q-TOF mass spectra (Fig. 2), these data suggest a choline-phosphate-6-Galf-Man-Man sequence.

NMR analysis of the five glycosphingolipid fractions

The GSL structures of *A. fumigatus* mycelium were elucidated by analysis of homonuclear and heteronuclear two-dimensional NMR experiments.

In agreement with GLC and MS data (Table I), NMR analysis confirmed the presence of an identical ceramide structure in all GSL fractions. From signal integration in the 1D spectrum of the highest concentrated GSL-B fraction, the total number of carbons of the two aliphatic chains was estimated to be 42. A methylene/methyl ratio of 17.5 was in agreement with a $C_{18:0}$ phytosphingosine linked to an unbranched 2-hydroxylated $C_{24:0}$ fatty acid identified by GLC-MS. The carbon linked to the nitrogen atom in the sphingosine base shifted at 53.36ppm was located in the ^{1}H ^{13}C HSQC experiment as well as three $^{1}H/^{13}C$ shifts corresponding to CHOH groups at 3.451/76.01, 3.348/73.65 and 3.835/74.3 (Fig. 4). A phosphorus atom was detected in the ceramide moiety attached to the glycosidic one. Indeed, three correlations were observed in the $^{1}H,^{31}P$ HSQC spectrum between the phosphorus atom and two methylene protons of the ceramide on one side and the H1 proton of inositol on the other side (Fig. 3, 4, 5) indicating the sequence inositol-P-ceramide.

GSL-U fraction

The chemical shifts and coupling constants of the glycosidic moiety obtained for the GSL-U fraction are shown in Table III. The 1D ^{1}H and 2D ^{1}H, ^{13}C gHSQC spectra showed three signals in the anomeric region, in equal proportions as deduced from integration in the 1D spectrum, indicating the presence of three monosaccharide residues (Fig. 3). The ^{1}H and ^{13}C chemical shift analysis and the examination of $^{3}J_{H,H}$ and $^{1}J_{C1,H1}$ values indicated the presence

of 2 α-mannopyranose and one α-glucosamine residues (Bock and Pedersen, 1974; 1983). The *myo*-inositol residue was identified from its H2 equatorial proton in the 1,2,3,4,5,6-cyclohexanehexol ring as assessed by the small $^{3}J_{H1,H2}$ and $^{3}J_{H2,H3}$ values (2,7Hz)(Table III).

A NOESY experiment demonstrated a strong correlation between the H1 proton of a mannose residue with the H3 proton of the second mannose residue (Fig. 3). Moreover, C1/H3 and H1/C3 correlations between these two mannose residues were observed in the gHMBC experiment (Fig. 3), indicating a branched sequence of α-Manp-(1→3)-α-Manp. This sequence accounts for the downfield chemical shift of the C3 at 82.24 ppm of the second mannose residue (Table III). Similarly, dipolar interactions between the H1 proton of the second mannose residue and H6/H6' protons of the glucosamine residue were observed in the NOESY experiment suggesting a →3)-α-Manp-(1→6)-α-GlcNH$_2$ sequence. This linkage was confirmed by an gHMBC experiment with the observation of the correlations H1/C6 and C1/H6H6' between the second mannose residue and the glucosamine residue. This is in agreement with a C6 downfield chemical shift at 68.29ppm observed for the glucosamine residue. A strong interaction was also observed in the NOESY experiment between the anomeric proton of the glucosamine residue and the H2 proton of the inositol residue, corroborated by the presence in the gHMBC experiment of a correlation between the C1 carbon of the glucosamine residue and the H2 proton of the inositol residue, indicating the sequence motif: →6)-α-GlcNH$_2$-(1→2)-Ins, in agreement with the downfield shift at 85.22 ppm of the inositol C2 carbon. Along with the MS data, the NMR experiments established the following structure: α-Manp-(1→3)-α-Manp-(1→6)-α-GlcNH$_2$-(1→2)-Ins-(1→O)-P-Cer. This structure has previously been characterized by NMR (Toledo *et al*., 2007). Differences in ^{1}H and ^{13}C chemical shifts are observed with our results that are associated primarily with the following: i) the ^{13}C referencing method inducing a shift of 3.11ppm, ii) the protonation state of the amine group of the glucosamine residue (Bunel *et al*., 1993).

GSL-B fraction.

Among the acidic GIPCs, fractions B was analysed first because it was the most abundant; it contained only one GSL spot on HPTLC (Fig. 1). The chemical shifts and coupling constants of the glycosidic moiety obtained for the GSL-B fraction are shown in Table IV. The 1D ^{1}H and 2D $^{1}H,^{13}C$ gHSQC spectra exhibited three signals of equivalent areas in the anomeric region (5.029/103.85ppm, 5.020/101.71ppm and 4.881/108.70ppm) indicating the presence of three monosaccharide residues (Fig. 4, Table IV). For the two first glycosidic residues, protons were assigned from anomeric proton only up to H3 and H4 respectively using relayed COSY experiments. The missing ring protons partly located in the TOCSY experiment were fully identified using the combination of ^{1}H, ^{13}C edited HSQC and H2BC experiments recently described as a useful method for tracing the proton-bearing carbon skeleton of a molecule (Petersen *et al*., 2006). Sugar rings stereochemistry deduced from $^{3}J_{H,H}$ coupling constants were consistent with Manp for these two glycosidic residues. Their α-configuration was evident from $^{1}J_{C1,H1}$ coupling constant values (169.1 and 173.1Hz). According to the GLC composition and methylation analysis (Tables I and II), the galactose residue was identified in a β-furanosic configuration by its characteristic very low field anomeric ^{13}C resonance at 108.70ppm (Ritchie *et al*., 1975). The *myo*-inositol residue was identified as previously for the GSL-U fraction. The NMR structural analysis of this fraction explicitly indicated the presence of two α-mannose, one β-galactofuranose and one inositol residues (Table IV).

In the NOESY spectrum, the two inter-residue dipolar interactions observed between the H1 proton of the β-galactofuranose residue and the H1 and H2 protons of a mannose residue did not allow the characterization of a branching point. In the gHMBC spectrum, only H1/C2 and C1/H2 inter-residues correlations between the β-galactofuranose residue and this mannose residue were observed indicating the β-Galf-(1→2)-α-Manp motif (Fig. 4). This linkage

accounts for the downfield chemical shift of the mannose C2 carbon at 77,08 ppm. In the NOESY spectrum, the H1/H3 interaction between the latter mannose residue and the second mannose residue indicates a →2)-α-Manp-(1→3)-α-Manp linkage. This glycosidic sequence was confirmed by H1/C3 and C1/H3 correlations between these two mannose residues observed in the gHMBC experiments but also by the downfield chemical shift of C3 of the second mannose residue at 81.70ppm (Table IV). The strong H1/H2 interaction between the second mannose residue and the inositol residue observed in the NOESY spectrum and the double correlation H1/C2 and C1/H2 observed in the gHMBC experiment between these two residues indicate the following sequence motif: →3)-α-Manp-(1→2)-Ins (Fig. 4). This is in agreement with the downfield shift of the inositol C2 carbon resonating at 80.91 ppm (Table IV). Together with methylation and MS data (Fig. 2, Table I), these NMR data established the structure of GSL-B as β-Galf-(1→2)-α-Manp-(1→3)-α-Manp-(1→2)-Ins-(1→O)-P-Cer.

GSL-A fraction.

In agreement with the TLC data, two distinct molecules were observed by NMR in the GSL-A fraction. The chemical shifts and coupling constants of the corresponding glycosidic sequences are shown in Table V. The one-dimensional ^{1}H spectrum (not shown) exhibited three signals in the anomeric region with areas in the ratio 2/1.2/2. The sugar spin systems assignment and the sequential glycosidic analysis revealed that these signals correspond to five protons belonging to two different molecules present in about equivalent amounts. The GSL-A2 molecule was identical to the GSL-B one. The GSL-A1 structure displayed the identical dimannoside core as GSL-A2 without the β-galactofuranose residue at the non-reducing end. Thus, the C2 carbon resonance of the first mannose residue was not downfield shifted for the GSL-A1 molecule (73.47ppm) upon branching of galactofuranose as observed for the GSL-A2 molecule (77.09ppm). Moreover, only three correlations were observed in the

^{1}H, ^{31}P HSQC (not shown) between a phosphorus atom (3.099ppm) and the two methylene protons of the ceramide on one side (4.039ppm and 3.658ppm) and the H1 proton of inositol on the other side (3.738ppm). These data are in agreement with the fact that the two molecules differ only at the non-reducing end of the glycosidic moiety. These NMR experiments indicated the presence of the two following structures: GSL A1, α-Manp-(1→3)-α-Manp-(1→2)-Ins-(1→O)-P-Cer and GSL A2, β-Galf-(1→2)-α-Manp-(1→3)-α-Manp-(1→2)-Ins-(1→O)-P-Cer

GSL-C fraction.

In this fraction, two different molecules were also observed which differ in their glycosidic sequences (Table VI). The presence of two different molecules was also confirmed by the observation of two close sets of three correlations in the ^{1}H, ^{31}P HSQC spectrum (data not shown) corresponding to two distinct phosphorus atoms resonating at 2.478ppm and 2.370ppm and interacting with the two methylene protons of the ceramide (δ=4.002 –3.667 ppm and δ=3.997 –3.670 ppm respectively) and the H1 proton of *myo*-inositol at 3.720ppm and 3.713ppm, respectively. The one-dimensional ^{1}H-NMR spectrum (not shown) exhibited eight H1 resonances of about equal intensity. In the anomeric region of the 2D $^{1}H,^{13}C$ gHSQC spectrum (not shown), six resonances among the eight were grouped two by two that resembled the anomeric region of the GSL-B fraction. Indeed, the sugar spin systems assignment and the sequential glycosidic analysis corresponded to the same glycosidic sequence which is β-Galf-(1→2)-α-Manp-(1→3)-α-Manp-(1→2)-Ins. One of the other anomeric signals at 4.799/111.10 ppm corresponded to a second β-galactofuranose residue identified by its characteristic downfield shifted anomeric carbon. The last anomeric signal at 4.640/102.57ppm was assigned to a α-mannopyranose residue. The $^{1}H,^{13}C$ edited gHSQC methylene region of the GSL-C fraction compared to that of the GSL-B fraction showed two

extra downfield shifted C6 at 68.27ppm and 69.79ppm indicating that the two corresponding mannose residues were 6-O-substituted.

Thus, NMR data allowed the identification of the two following molecules :

GSL-C1, β-Galf(1→2)-α-Manp(1→3)-[α-Manp(1→6)]-α-Manp-(1→2)-Ins(1→O)-P-Cer and GSL-C2, β-Galf(1→2)-α-Manp(1→3)-[β-Galf(1→6)]-α-Manp-(1→2)-Ins(1→O)-P-Cer.

GSL-D fraction.

The chemical shifts and coupling constants obtained for this fraction are summarized in Table VII. The 1D ^{1}H and 2D $^{1}H,^{13}C$ gHSQC spectra exhibited three signals of equivalent areas in the anomeric region (5.108/103.47ppm, 5.069/102.24ppm and 4.939/109.11ppm), indicating the presence of three monosaccharides (Fig. 5). The glycosidic ring spin systems assignment and coupling constants examination permitted the identification of two α-mannose residues and one β-galactofuranose residue as in the GSL-B fraction. Moreover, the NOESY and gHMBC spectra showed the same inter-residue connectivities as those observed for the GSL-B fraction (Fig. 4 and 5), emphasizing the monosaccharide sequence identity with GSL-B. However, differences were observed when comparing $^{1}H,^{13}C$ HSQC spectra of the two fractions (Fig. 4 and 5). Thus, a large downfield shift at 68.92ppm and a smaller upfield shift at 72.11ppm were observed for the C6 and C5 carbons respectively of the β-Galf residue for the GSL-D fraction, indicating a 6-O substitution for this residue. Furthermore, in a gHSQC experiment, two new methylene carbons and one trimethyl group have been identified at 4.127/61.62ppm, 3.571/68.79ppm and 3.169/56.48ppm respectively. The COSY experiment showed that these methylene carbons were linked together. The characteristic methyl ^{13}C shift is consistent with the MS data (Fig. 2), indicating the presence of an N-trimethyl group (Fig. 5). In the HMBC spectrum, two $^{1}H,^{13}C$ long range interactions were observed between this N-trimethyl group and the second methylene group indicating the presence of the $(CH_3)_3$-N-

CH_2-CH_2 motif. Two sets of correlations were observed in the $^{1}H,^{31}P$ HSQC (Fig. 5). A first set of three correlations was detected between a phosphorus atom (2.974ppm) and the two methylene protons of the ceramide on one side (4.094ppm and 3.660ppm) and the H1 proton of inositol on the other side (3.756ppm), corresponding to the IPC. Another set of two correlations was observed between a second phosphorus atom (0.763ppm) and the two extra methylene protons on the one hand (4.127ppm) and the H6 protons of β-Galf on the other hand (3.764ppm). This was in agreement with the chemical shifts observed for C6 and C5 carbons resonances of the β-Galf residue, indicating its substitution by a phosphocholine residue. In addition, the comparison with the ^{1}H 1D and $^{1}H,^{13}C$ HSQC spectra of a phosphatidylcholine reference compound (Sigma) confirmed the resonances assignment of the phosphocholine (not shown). Thus, the NMR analysis, in agreement with methanolysis/trimethylsylation, methylation and MS data, showed that the GSL-D fraction corresponded to Cho-P-(O→6)-β-Galf-(1→2)-α-Manp-(1→3)-α-Manp-(1→2)-Ins(1→O)-P-Cer. The substitution of galactofuranose residue by a phosphate group explanes the low amont of galactose detected by GLC (Table 1).

Discussion

The results presented here and in previous studies show that *A. fumigatus* produced at least 9 GIPCs of different structure (Table VIII). All GSLs have the same ceramide moiety composed of a 2-hydroxylated lignoceric acid (2-OH $C_{24:0}$) associated with a $C_{18:0}$-phytosphingosine base. This lipid moiety is common to most fungi species. The glycan part has more variability and 2 types of GIPC have been isolated from *A. fumigatus* mycelium. First, a zwitterionic GSL that is the major GIPC from *A. fumigatus* mycelium contains a glucosamine residue linked in α1-2 to the inositol ring. This unusual carbohydrate sequence has been recently described in *A. fumigatus* by Toledo and his colleagues (Toledo *et al.*, 2007)

and has been described in only two other fungal pathogens, *S. schenckii and Acremonium sp*. (Toledo *et al*., 2001a; Aoki *et al*., 2004a). Secondly, the 5 other acidic GSL structures contain a common sequence α-Man-(1-3)-α-Man-(1-2)-Inositol. This sequence has been previously described in *A. fumigatus* GSL (Levery *et al*., 2001; Toledo *et al*., 2007) and other fungal species (Levery *et al.*, 1998; 2001; Bennion *et al*., 2003; Barr *et al*., 1984). No α-Man-(1-6)-Inositol as found in *S. schenckii* (Toledo *et al*., 2001a; Loureiro y Penha *et al*., 2001) and no α-Man-(1-4)-Inositol as found in mushrooms (Jennemann *et al.*, 1999) have been observed in *A. fumigatus* GSLs. Four of the five acidic GSLs analysed contained galactofuranose in *A. fumigatus*. The presence of galactofuranose in GSLs has been reported in human pathogens such as *Histoplasma capsulatum, Paracoccidioïdes brasiliensis, A. fumigatus* (Barr *et al*., 1984; Levery *et al*., 1998, Toledo *et al*., 2007). In these later structures, the galactofuranose residue is linked to the first mannose like for the GSL-C2 of *A. fumigatus*. However, the galactofuranose residue is mainly linked to the terminal non-reduced mannose residue through a β1-2 linkage (GSL-B). Surprisingly, a choline-phosphate group has been localized to the terminal galactofuranose residue (GSL-D). A choline phosphate in a GSL structure has also been found in *Acremonium sp.*, however it is linked to a mannose residue instead of a galactofuranose residue (Aoki *et al*., 2004a). Some discrepancies are seen between our data and the study of Toledo (Toledo *et al*., 2007). These authors did not observe the β−galactofuranose linked in β1-2 to the terminal mannose and the choline-phosphate linked to this β−galactofuranose. In contrast, they described the presence of a mannose residue linked in α1-2 to Man_2-IPC that we did not observe. These differences are not explained and could be due to the use of different growth conditions or to different strains.

GIPCs have been mainly analysed in human fungal pathogens (*A. niger, H. capsulatum, P. brasiliensis, S. schenckii, C. neoformans*), and it has been suggested that GIPCs have an immunological function during fungal infection. The presence of

galactofuranose in these GIPCs that is absent in mammals, seems to play an important role in fungal-host interactions. Earlier studies have shown that galactofuranose containing molecules of *A. fumigatus* are extremely antigenic (Latgé *et al*., 1994; Costachel *et al*., 2005; Morelle *et al*, 2005; Leitao *et al*., 2003). Galactofuranose residues are also an immunodominant in GSLs of *P. brasiliensis* and *H. capsulatum* (Barr and Lester, 1984; Levery *et al*., 1998). In *Leishmania major*, a monoclonal antibody against a glycolipid containing terminal galactofuranose residue can reduce the macrophage infectivity of this parasite (Suzuki *et al*., 2002). The expression in infected human tissues of intelectin that recognizes a single terminal galactofuranose residue (Tsuji *et al*., 2001) is in agreement with the involvement of galactofuranosylated GSLs during infection. Antibodies from patients with aspergillosis recognized the *A. fumigatus* GIPCs isolated by Toledo *et al*. (2007), however, the role of *A. fumigatus* GIPCs in host cellular immunity has not been defined as yet.

The biosynthetic pathway of sphingolipids begins in the endoplasmic reticulum where it proceeds to the formation of the ceramide moiety. A linkage between the carbohydrate and phytosphingosine occurs in the Golgi apparatus (Funato *et al*., 2002; Dickson *et al*., 2006). In yeast, ceramide biosynthesis and inositol addition are essential for growth. Indeed, GIPCs are involved in cell regulation, cell polarity, stress response, trafficking and cell wall integrity (Dickson *et al*. 2006). Similarly, in *Aspergillus*, the gene encoding the IPC synthase is essential for fungal growth as well as basA gene-encoding a phytosphingosine (Li *et al*., 2007). Sphingolipids are involved in polarised growth via the control of actin cytoskeleton (Cheng *et al*., 2001; Hu *et al*., 2007). This result is in agreement with the susceptibility of *Aspergillus* species to various inhibitors of sphingolipid synthesis pathway (Zhong *et al*., 2000; Li *et al*., 2007). In *A. fumigatus*, 3 types of membrane anchored molecules present the same inositol-phosphoceramide lipid moiety: GPI-anchored protein (Fontaine *et al*., 2003);

the lipogalactomannan, a GPI-anchored polysaccharide (Costachel *et al*., 2005) and GIPCs. In this study, the inositol ring of IPC structure could be substituted in position 2 by a mannose or a glucosamine residue. In contrast, previous studies suggested that the glucosamine residue is linked in α1-6 to the inositol ring in the GPI-anchor structures from GPI-protein or from the lipogalactomannan

In *S. cerevisiae*, 2 homologous genes of IPC mannosyltransferases are involved in the addition of the first mannose residue to the inositol ring. The deletion of both genes is not lethal, but mutants are sensitive to the external Ca^{2+} (Beeler *et al*., 1997), suggesting a role for the GSLs in cellular stress response. In *C. albicans*, the deletion of the MIT1, an IPC mannosyltransferase homologue induced the absence of MIPC, M(IP)2C and the phospholipomannan (β1-2mannan linked to MIPC) and decreased virulence of the mutant (Trinel *et al*., 2002; Mille *et al*., 2004). In *A. fumigatus*, no such mutant has been described, so the relevance of these GIPCs during *A. fumigatus* growth and host-pathogen interactions is still unknown.

Materials and methods

Fungal culture and membrane preparation

A. fumigatus, strain CBS 144-89 was grown in a 15-L fermenter in 2% glucose and 1% mycopeptone (Biokar Diagnostics, Pantin, France) for 24 h at 25°C as described previously (Hartland *et al.* 1996). The mycelium was collected by filtration under vacuum, washed with water, and then disrupted in 200 mM TrisHCl, 20 mM EDTA, pH 8.0, 1 mM PMSF buffer at 4°C with glass beads (1 mm, diameter) in a Dyno mill apparatus (W. A. Bachofen AG, Basel, Switzerland). The cell wall was removed by centrifugation at 10,000 g 10 min at 4°C. Total membranes were then collected by ultracentrifugation at 125,000 g 60 min at 4°C. Membrane pellet was homogenized in the disruption buffer with a Dounce homogenizer and then

centrifuged once more at 125,000 g for 60 min at 4°C. Pellet was resuspended again in 20 mM TrisHCl, 2 mM EDTA, pH 8.0 and store at -80°C.

Extraction and purification of glycosylinositolphosphatidylceramides

A chloroform/methanol mixture was added to the membrane suspension (20 mg of protein/ml) to obtain a chloroform/methanol/membrane ratio of 10/10/3 respectively. The mixture was stirred for 2 h at room temperature, then centrifuged at 10,000 g for 10 min. The pellet was resuspended in a chloroform/methanol/water (10/10/3, v/v/v) mixture, and the extraction was repeated once. Pooled supernatants were concentrated under vacuum with a rotavapor, and the residue was submitted to a butanol/water partition. The water phase containing GIPCs was dialysed against water and freeze-dried. The residue was dissolved in chloroform/methanol/water (10/15/4, v/v/v) and applied onto a DEAE-Sephadex A-25 column (Pharmacia, 2 x 15 cm) equilibrated in the same solvent at the flow rate of 30 ml/h. Unbound products were eluted with 2 column volumes of solvent, then retained products were eluted by a chloroform/methanol/NH_4Ac 1M (10/15/4) solvent. Carbohydrates were detected by spraying with orcinol sulfuric acid on spot of 2 µl of different fractions on silica sheets. Fractions containing sugars were concentrated and then dialysed against water and freeze-dried. GIPCs were then purified on a silica 60 column (Merck, 1.8 x 30 cm) equilibrated in propanol-1/water/NH_4OH 30% (85/15/5, v/v/v) and eluted at 25ml/h. Samples were deposited onto the silica 60 column and eluted by 3 column volumes of propanol-1/water/NH_4OH 30% (85/15/5, v/v/v), then 3 volumes of propanol-1/water/NH_4OH 30% (80/20/5, v/v/v), then 3 volumes of propanol-1/water/NH_4OH 30% (70/30/5, v/v/v). The presence of carbohydrate in the fraction was detected as described above. Fractions were dialysed against water and freeze-dried.

Analytical methods.

Neutral hexoses were identified by GLC as alditol acetates obtained after hydrolysis (4 N trifluoroacetic acid, 100°C, 4h.)(Sawardeker *et al*., 1967). Glucosamine and *myo*-inositol were quantified by GLC-MS after hydrolysis (6 N HCL, 110°C 20h), N-acetylation and trimethysilyation, using the *scyllo*-inositol as a standard (Ferguson, 1993). Lipid analysis was performed by GLC-MS on HF-treated GIPC fraction (aqueous 50% HF, 2 days on ice). Fatty acids and sphingosine bases were released by methanolysis (1 N HCl in MeOH, 80°C, 20h). Fatty acids were extracted with heptane and analysed after trimethylsilylation. The methanol phase containing the sphingosine base was N-acetylated, trimethylsilylated and analysed by GLC-MS. Phosphorylated carbohydrates were identified by GLC-MS after acid methanolysis (1 N HCL in methanol, 80°C, 20h) and trimethylsilylation (Ferguson, 1993). The lipophosphoglycan from *Leishmania donovani,* a kind gift from Pascale Pescher (Unité de Virulence Parasitaire, Institut Pasteur) was used as positive control. Methylation of GSL fractions was performed using the sodium hydroxide procedure (Ciucanu and Kerek, 1984). GSL containing a glucosamine residue was peracetylated with a pyridine/acetic anhydride solution (50/200 µl) overnight at room temperature prior to the methylation procedure. Methyl ethers were analysed by GLC-MS as polyolacetates (Björndal *et al*., 1970).

HPTLC. GIPC fractions were applied to a 10 cm aluminium-backed silica gel 60 (Merck) and developed with chloroform/methanol/1 M ammonium acetate/NH_4OH 30%/water (180/140/9/9/23). Sugars were detected with orcinol-sulfuric acid.

GLC and GLC-Mass spectrometry. GLC was performed on a Delsi 200 instrument with a flame ionisation detector using a capillary column (30 m x 0.25 mm id) filled with a EC^{TM}-1 (Alltech) under the following conditions: gas vector and pressure, helium 0.7 bar; temperature

program 120 to 180°C at 2°C/min and 180 to 240°C at 4°C/min. GLC-MS was performed on an Automass II apparatus (Finigan) coupled to a CarloErba gas chromatograph (model 8000top), using a capillary column (30 m x 0.25 mm id) filled with a EC^{TM}-1 (Alltech) under the following conditions : gas vector and flow rate, helium 1.2 ml/min; temperature program for inositol and monosaccharide analysis : 100 to 200°C at 5°C/min, 200 to 240°C at 15°C/min and 240°C for 5 min; temperature program for sphingosine base and fatty acid analysis : 100 to 200°C at 10°C/min, 200 to 260°C at 15°C/min and 260°C for 13 min.

Nano-electrospray mass spectrometry. Mass spectrometric analyses were performed in the negative mode using a Q-STAR Pulsar quadrupole time-of-flight (Q-TOF) mass spectrometer (AB/MDS Sciex, Toronto, Canada) equipped with a nano-electrospray ion source (Protana, Odense, Denmark).

The samples in propanol-1/H_2O (25/75) dissolved in chloroform/methanol (50/50) were sprayed from gold-coated 'medium length' borosilicate capillaries (Protana, Odense, Denmark). A potential of -800 V was applied to the capillary tip. The declustering potential was set at -120V and the focusing potential was set at -200V. The molecular ions were then selected in the quadrupole analyzer and partially fragmented in the hexapole collision cell, with the pressure of collision gas (N_2) 5.3 x 10^{-5} Torr (1Torr = 133.3 Pa). The collision energy was varied between -40 and -80 eV depending on the sample. For the recording of conventional mass spectra, TOF data were acquired by accumulation of 10 MCA (multiple channel acquisition) scans over mass ranges of m/z ranges 500-1800 Daltons for MS analyses and over mass ranges of m/z 50-1800 for MS/MS analyses. Data acquisition was optimized to supply the highest possible resolution and the best signal-to-noise ratio, even in the case of low abundance signals. Typically, the FWHM (full width at half maximum) was 7000 in the measured mass ranges. External calibration was performed prior to each measure using a

4 pmol/µl solution of taurocholic acid in acetonitrile/water (50/50, v/v) containing 2 mM of ammonium acetate.

NMR Spectroscopy. NMR spectra were acquired at 50°C on a Varian Inova 500 spectrometer equipped with a triple $^{1}H\{^{13}C/^{15}N\}$ resonance ^{1}H PFG probe or an indirect PFG probe for ^{1}H, ^{31}P experiments. For the low concentration samples, complementary experiments were performed at 35°C on a Varian Inova 600 spectrometer equipped with a cryogenically-cooled triple resonance $^{1}H\{^{13}C/^{15}N\}$ PFG probe. Samples were dissolved in DMSO-d6 for NMR (99.96% ^{2}H atoms, Euriso-top, CEA, Saclay, France) and transferred in 5mm Shigemi tubes (Shigemi Inc., Alison Park, United States). D_2O (99.97% 2H atoms, Euriso-top, CEA, Saclay, France) was added in order to exchange sugars hydroxyl protons. Since the proton chemical shift of the residual signal of DMSO-d6 depends on temperature and water content, external referencing was applied for ^{1}H chemical shifts using a capillary containing a freshly prepared solution of 20 mM DSS in DMSO-d6 containing less than 0,01% of water. The DSS methyl resonance was set to 0ppm. ^{13}C chemical shifts were then calculated from ^{1}H chemical shift and gamma ratio relative to DSS. $^{13}C/^{1}H$ gamma ratio of 0.251449530 was used (Wishart *et al.*, 1995). ^{31}P chemical shifts were determined with neat phosphoric acid (Wilmad-Labglas, New Jersey, USA) by substitution method.

For all GSL fractions, the same general strategy was adopted for assignment of nuclei. First, the proton resonances were assigned using two-dimensional COSY and RELAY experiments with one to three relays to follow connectivities from the anomeric proton up to the H5 proton of most of glycosidic residues (Rance *et al.*, 1983; Wagner 1983). The intra glycosidic residue spin systems were often completed by mean of a TOCSY experiment with a long mixing time (120ms) (Griesinger *et al.*, 1988). A ^{1}H-^{13}C edited gHSQC experiment allowed to achieve ^{13}C chemical shifts assignment from previously identified ^{1}H resonances (Willker *et al.*, 1993).

Then, $^{1}H,^{1}H$ coupling constants analysis from 1D and/or COSY spectrum (^{1}H resolution of 0.1 Hz and 1,6Hz respectively) was used to assess the identity of monosaccharide residues. Moreover, the anomeric configuration of monosaccharide residues was established from knowledge of $^{3}J_{1,2}$ values and confirmed by the measurement of the $^{1}J_{C1H1}$ heteronuclear coupling constants in the ^{1}H dimension of the undecoupled gHSQC spectrum (^{1}H resolution of 0.6Hz) or of the gHMBC spectrum (^{1}H resolution of 1.2Hz) (Willker *et al.*, 1993). Finally, glycosidic linkages were established via through-space dipolar interactions using ^{1}H-^{1}H NOESY experiment (mixing time of 200ms) (Macura *et al.*, 1981) and/or via three-bond interglycosidic ^{1}H-^{13}C correlations using ^{1}H-^{13}C gHMBC experiment (long range delay of 60ms). In addition, the branching point between the phospholipid and the glycosidic moieties was identified using the ^{1}H-^{31}P gHSQC.

Acknowledgments

We thank Professor R. Calderone (Georgetown University Medical center, Washington, USA) for reading of the manuscript.

Abbreviations

COSY: Correlation spectroscopy

DMSO: Dimethylsulfoxyde

DSS: 2,2-dimethyl-2-silapentane- 5-sulfonate sodium salt

GIPC: Glycosylinositolphosphoceramide

GLC: Gas-liquid chromatography

GLC-MS: Gas-liquid chromatography-mass spectrometry

GPI: Glycosylphosphatidylinositol

GSL: Glycosphingolipid

H2BC: Heteronuclear two-bond correlation

gHMBC: Gradient selected heteronuclear multiple bond correlation

gHSQC: Gradient selected heteronuclear single-quantum correlation

HPTLC: High performance thin layer chromatography

IPC: Inositolphosphoceramide

MS: Mass spectrometry

NMR: Nuclear magnetic resonance

NOESY: Nuclear overhauser effect spectroscopy

Q-TOF: Pulsar quadrupole-time of flight

RELAY 2D: Relayed COSY

PFG: Pulsed field gradient

TOCSY: Total correlation spectroscopy

References

Aoki K, Uchiyama R, Itonori S, Sugita M, Che FS, Isogai A, Hada N, Hada J, Takeda T, Kumagai H, Yamamoto K. 2004a. Structural elucidation of novel phosphocholine-containing glycosylinositol-phosphoceramides in filamentous fungi and their induction of cell death of cultured rice cells. Biochem J. 378:461-472.

Aoki K, Uchiyama R, Yamauchi S, Katayama T, Itomori S, Sugita M, Hada N, Yamada-Hada J, Takeda T, Kumagai H, Yamamoto K. 2004b. Newly discovered neutral glycosphingolipids in aureobasidin A-resistant *Zygomycetes*. J. Biol. Chem. 279:32028-32034.

Arigi E, Singh S, Kahlili AH, Winter H. C, Goldstein IJ, and Levery SB. 2007. Characterization of neutral and acidic glycosphingolipids from the lectin-producing mushroom, *Polyporus squamosus*. Glycobiology 17:754-766.

Barr K, Lester RL. 1984. Occurrence of novel antigenic phosphoinositol-containing sphingolipids in the pathogenic yeast *Histoplasma capsulatum*. Biochemistry. 23:5581-5588.

Beeler TJ, Fu D, Rivera J, Monaghan E, Gable K, Dunn TM. 1997. *SUR1 (CSG1/BCL21)*, a gene necessary for growth of *Saccharomyces cerevisiae* in the presence of high Ca2+ concentrations at 37 degrees C, is required for mannosylation of inositolphosphorylceramide. Mol Gen Genet. 255:570-579.

Bennion B, Park C, Fuller M, Lindsey R, Momany M, Jennemann R, Levery SB. 2003. Glycosphingolipids of the model fungus *Aspergillus nidulans*: characterization of GIPCs with oligo-alpha-mannose-type glycans. J Lipid Res. 44:2073-2088.

Björndal H, Hellerqvist CG, Lindberg B, Svensson S. 1970. Gas-liquid chromatography and mass spectrometry in methylation analysis of polysaccharides. Angew. Chem. Int.9:610-619.

Bock K, Pedersen C. 1974. A study of ^{13}CH coupling constants in hexopyranoses. J Chem Soc Perkin Trans. II:293-297.

Bock K, Pedersen C. 1983. Carbon-13 nuclear magnetic resonance spectroscopy of monosaccharides. Adv. Carbohydr. Chem. Biochem. 41:27-44.

Bunel S, Ibarra C, Moraga E, Blasko A, Bunton CA. 1993. Structures of complexes of cobalt(III) and glucosamine. Applications of molecular mechanics and NMR spectroscopy. Carbohydr. Res. 244:1-14.

Cheng J, Park TS, Fischl AS, Ye XS. 2001. Cell cycle progression and cell polarity require sphingolipid biosynthesis in *Aspergillus nidulans*. Mol Cell Biol. 21:6198-6209.

Ciucanu I, Kerek F. 1984. A simple and rapid method for the permethylation of carbohydrates. Carbohydr. Res. 131:209-217.

Costachel C, Coddeville B, Latgé JP, Fontaine T. 2005. Glycosylphosphatidylinositol-anchored fungal polysaccharide in *Aspergillus fumigatus*. J Biol Chem. 280:39835-39842.

da Silva AF, Rodrigues ML, Farias SE, Almeida IC, Pinto MR, Barreto-Bergter E. 2004. Glucosylceramides in *Colletotrichum gloeosporioides* are involved in the differentiation of conidia into mycelial cells. FEBS Lett. 561:137-143.

Dickson RC, Sumanasekera C, Lester RL. 2006. Functions and metabolism of sphingolipids in *Saccharomyces cerevisiae*. Prog Lipid Res. 45:447-465.

Ferguson MA. 1993. GPI-membrane anchors: isolation and analysis in Glycobiology, a practical approach. ed. M Fukudo, A Kobata, pp. 349-383: Oxford University, IRL Press

Fontaine T, Magnin T, Melhert A, Lamont D, Latgé JP, Ferguson MA. 2003. Structures of the glycosylphosphatidylinositol membrane anchors from *Aspergillus fumigatus* membrane proteins. Glycobiology. 13:169-177.

Funato K, Vallee B, Riezman H. 2002. Biosynthesis and trafficking of sphingolipids in the yeast *Saccharomyces cerevisiae*. Biochemistry. 41:15105-15114.

Griesinger C, Otting G, Wüthrich K, Ernst RR. 1988. Clean TOCSY for proton spin system identification in macromolecules. J. Am. Chem. Soc. 110:7870-7872.

Gutierrez A. LS, Farage L, Melo M. N, Mohana-Borges R. S, Guerardel Y, Coddeville B, Wieruszeski J-M, Mendonça-Previato L, Previato J. O. 2007. Characterization of glycoinositolphosphoryl ceramide structure mutant strains of *Cryptococcus neoformans*. Glycobiology 17:1C-11C.

Hartland RP, Fontaine T, Debeaupuis JP, Simenel C, Delepierre M, Latgé JP. 1996. A novel beta-(1-3)-glucanosyltransferase from the cell wall of *Aspergillus fumigatus*. J Biol Chem. 271:26843-26849.

Heise N, Gutierrez AL, Mattos KA, Jones C, Wait R, Previato JO, Mendonca-Previato L. 2002. Molecular analysis of a novel family of complex glycoinositolphosphoryl ceramides from *Cryptococcus neoformans*: structural differences between encapsulated and acapsular yeast forms. Glycobiology. 12:409-420.

Hu W, Sillaots S, Lemieux S, Davison J, Kauffman S, Breton A, Linteau A, Xin C, Bowman J, Becker J, Jiang B, Roemer T. 2007. Essential Gene Identification and Drug Target Prioritization in *Aspergillus fumigatus*. PLoS Pathog. 3:e24.

Jennemann R, Bauer BL, Bertalanffy H, Geyer R, Gschwind RM, Selmer T, Wiegandt H. 1999. Novel glycoinositolphosphosphingolipids, basidiolipids, from *Agaricus*. Eur J Biochem. 259:331-338.

Jennemann R, Geyer R, Sandhoff R, Gschwind RM, Levery SB, Grone HJ, Wiegandt H. 2001. Glycoinositolphosphosphingolipids (basidiolipids) of higher mushrooms. Eur J Biochem. 268:1190-1205.

Latgé JP. 1999. *Aspergillus fumigatus* and aspergillosis. Clin Microbiol Rev. 12:310-350.

Latgé JP, Kobayashi H, Debeaupuis JP, Diaquin M, Sarfati J, Wieruszeski JM, Parra E, Bouchara JP, Fournet B. 1994. Chemical and immunological characterization of the extracellular galactomannan of *Aspergillus fumigatus*. Infect Immun. 62:5424-5433.

Leitao EA, Bittencourt VC, Haido RM, Valente AP, Peter-Katalinic J, Letzel M, de Souza LM, Barreto-Bergter E. 2003. Beta-galactofuranose-containing *O*-linked oligosaccharides present in the cell wall peptidogalactomannan of *Aspergillus fumigatus* contain immunodominant epitopes. Glycobiology. 13:681-692.

Levery SB, Momany M, Lindsey R, Toledo MS, Shayman JA, Fuller M, Brooks K, Doong RL, Straus AH, Takahashi HK. 2002. Disruption of the glucosylceramide biosynthetic pathway in *Aspergillus nidulans* and *Aspergillus fumigatus* by inhibitors of UDP-Glc:ceramide glucosyltransferase strongly affects spore germination, cell cycle, and hyphal growth. FEBS Lett. 525:59-64.

Levery SB, Toledo MS, Straus AH, Takahashi HK. 1998. Structure elucidation of sphingolipids from the mycopathogen *Paracoccidioides brasiliensis*: an immunodominant beta-galactofuranose residue is carried by a novel glycosylinositol phosphorylceramide antigen. Biochemistry. 37:8764-8775.

Levery SB, Toledo MS, Straus AH, Takahashi HK. 2001. Comparative analysis of glycosylinositol phosphorylceramides from fungi by electrospray tandem mass spectrometry with low-energy collision-induced dissociation of Li(+) adduct ions. Rapid Commun Mass Spectrom. 15:2240-2258.

Loureiro y Penha CV, Todeschini AR, Lopes-Bezerra LM, Wait R, Jones C, Mattos KA, Heise N, Mendonca-Previato L, Previato JO. 2001. Characterization of novel structures of mannosylinositolphosphorylceramides from the yeast forms of *Sporothrix schenckii*. Eur J Biochem. 268:4243-4250.

Li S, Bao D, Yuen G, Harris SD, Calvo AM. 2007. *bas*A regulates cell wall organization and asexual/sexual sporulation ratio in *Aspergillus nidulans*. Genetics 176:243-253.

Maciel DM, Rodrigues ML, Wait R, Villas Boas MHS, Tischer CA, Barreto-bergter E. 2002. Glycosphingolipids from *Magnaporthe grisea* cells: expression of a ceramide dihexoside presenting phytosphingosine as the long-chain base. Arch. Biochem. Biophys. 405:205-213.

Macura S, Huang Y, Suter D, Ernst RR. 1981. Two-dimensional chemical exchange and cross-relaxation spectroscopy of coupled nuclear spins. J Magn Reson. 43:259-281.

Mille C, Janbon G, Delplace F, Ibata-Ombetta S, Gaillardin C, Strecker G, Jouault T, Trinel PA, Poulain D. 2004. Inactivation of CaMIT1 inhibits *Candida albicans*

phospholipomannan beta-mannosylation, reduces virulence, and alters cell wall protein beta-mannosylation. J Biol Chem. 279:47952-47960.

Morelle W, Bernard M, Debeaupuis JP, Buitrago M, Tabouret M, Latgé JP. 2005. Galactomannoproteins of *Aspergillus fumigatus*. Eukaryot Cell. 4:1308-1316.

Nagiec MM, Nagiec EE, Baltisberger JA, Wells GB, Lester RL, Dickson RC. 1997. Sphingolipid synthesis as a target for antifungal drugs. Complementation of the inositol phosphorylceramide synthase defect in a mutant strain of *Saccharomyces cerevisiae* by the AUR1 gene. J Biol Chem. 272:9809-9817.

Petersen BO, Vinogradov E, Kay W, Würtz P, Nyberg NT, Duus JO, Sorensen OW. 2006. H2BC: a new technique for NMR analysis of complex carbohydrates. Carbohydr Res. 341:550-556.

Rance M, Sorensen OW, Bodenhausen G, Wagner G, Ernst RR, Wüthrich K. 1983. Improved spectral resolution in COSY 1H NMR spectra of proteins via double quantum filtering. Biochem Biophys Res Commun. 117:479-485.

Ritchie RG, Cyr N, Korsch B, Koch HJ, Perlin A. 1975. Carbon-13 chemical shifts of furanosides and cyclopentanols. Configurational and conformational influences. Can. J. Chem. 53:1424-1433.

Rittershaus P, Kechichian TB, Allegood JC, Merril Jr AH, Hennig M, Luberto C, Del Poeta M. 2006. Glucosylceramide synthase in an essential regulator of pathogenicity of *Cryptococcus neoformans*. J. Clin. Investi. 116:1651-1659.

Sawardeker JS, Sloneker JH, Jeanes A. 1967. Quantitative determination of monosaccharides as their alditol acetates by gas liquid chromatography. Anal Chem. 37:1602-1604.

Suzuki E, Tanaka AK, Toledo MS, Takahashi HK, Straus AH. 2002. Role of beta-D-galactofuranose in *Leishmania major* macrophage invasion. Infect Immun. 70:6592-6596.

Toledo MS, Levery SB, Bennion B, Guimaraes LL, Castle SA, Lindsey R, Momany M, Park C, Straus AH, Takahashi HK. 2007. Sphingolipids of the mycopathogen *Aspergillus fumigatus*: characterization of glycosylinositol phosphorylceramide antigens with Manp(alpha 1-2)Ins and GlcpN(alpha 1-2)Ins core motifs. J. Lipid Res. 48:1801-1824.

Toledo MS, Levery SB, Glushka J, Straus AH, Takahashi HK. 2001a. Structure elucidation of sphingolipids from the mycopathogen *Sporothrix schenckii*: identification of novel glycosylinositol phosphorylceramides with core manalpha1-->6Ins linkage. Biochem Biophys Res Commun. 280:19-24.

Toledo MS, Levery SB, Straus AH, Takahashi HK. 2001b. Sphingolipids of the mycopathogen *Sporothrix schenckii*: identification of a glycosylinositol phosphorylceramide with novel core GlcNH(2)alpha1-->2Ins motif. FEBS Lett. 493:50-56.

Trinel PA, Maes E, Zanetta JP, Delplace F, Coddeville B, Jouault T, Strecker G, Poulain D. 2002. *Candida albicans* phospholipomannan, a new member of the fungal mannose inositol phosphoceramide family. J Biol Chem. 277:37260-37271.

Tsuji S, Uehori J, Matsumoto M, Suzuki Y, Matsuhisa A, Toyoshima K, Seya T. 2001. Human intelectin is a novel soluble lectin that recognizes galactofuranose in carbohydrate chains of bacterial cell wall. J Biol Chem. 276:23456-23463.

Wagner G. 1983. Two-dimensional relayed coherence transfer spectroscopy of a protein. J. Magn Reson. 55:151-156.

Willker W, Leibfritz D, Kerssebaum R, Bermel W. 1993. Gradient selection in inverse heteronuclear correlation spectroscopy. Magn Reson Chem. 31:287-292.

Wishart DS, Bigam CG, Yao J, Abildgaard F, Dyson HJ, Oldfield E, Markley JL, Sykes BD. 1995. 1H, 13C and 15N chemical shift referencing in biomolecular NMR. J Biomol NMR. 6:135-140.

Zhong W, Jeffries MW, Georgopapadakou NH. 2000. Inhibition of inositol phosphorylceramide synthase by aureobasidin A in *Candida* and *Aspergillus* species. Antimicrob Agents Chemother. 44:651-653.

Legends to figures

Figure 1: HPTLC of GSL fractions (U, A, B, C, D) isolated from *A. fumigatus* mycelium. TLC was developed on 10-cm aluminium-coated silica gel 60 with chloroform/methanol/1 M ammonium acetate/NH_4OH 30%/water (180/140/9/9/23). Sugars were detected using orcinol sulfuric acid.

Figure 2: Nano-electrospray mass spectrometry analysis of GSL-B and GSL-D fractions of *A. fumigatus* mycelium. Mass spectrometric analyses were performed in negative mode using a Q-STAR Pulsar quadrupole time-of-flight (Q-TOF) mass spectrometer equipped with a nano-electrospray ion source. A: negative ion mass spectrum; B: daughter ion mass spectrum of molecular ion.

Figure 3: NMR spectra of GSL-U isolated from *A. fumigatus* mycelium. ^{1}H-^{13}C HSQC, ^{1}H-^{1}H NOESY, ^{1}H-^{13}C HMBC and ^{1}H-^{31}P HSQC.

Figure 4: NMR spectra of GSL-B from *A. fumigatus* mycelium. ^{1}H-^{13}C HSQC, ^{1}H-^{1}H NOESY, ^{1}H-^{13}C HMBC and ^{1}H-^{31}P HSQC.

Figure 5: NMR spectra of GSL-D from *A. fumigatus* mycelium. ^{1}H-^{13}C HSQC, ^{1}H-^{1}H NOESY, ^{1}H-^{13}C HMBC and ^{1}H-^{31}P HSQC.

Table I. Carbohydrate composition and Q-TOF mass analysis of GSL fractions isolated from *A. fumigatus* mycelium

(Man : mannose; Gal : galactose; GlcN : glucosamine; IPC : inositolphosphoceramide; Hex : hexose; Cho-P : choline-phosphate)

	Monosaccharide composition *				Pseudomolecular ions identified by Q-TOF		
GSL Fractions	Man	Gal	GlcN	Inositol	Main ions	Corresponding structures	Minor ions
GSL-U	1	-	0.49	+	1409.8	Hex_2-GlcN-IPC	1424.1 ; 1437.8
GSL-A	1	0.36	-	+	1249.1; 1411.2	Hex_2-IPC ; Hex_3-IPC	1263.1 ; 1277.1 1425.2 ; 1439.2
GSL-B	1	0.49	-	+	1411.2	Hex_3-IPC	1425.2 ; 1439.2
GSL-C	1	0.42	-	+	1573.3	Hex_4-IPC	1587.3 ; 1601.3
GSL-D	1	0.11	-	+	1576.3	Cho-P-Hex_3-IPC	1590.3 ; 1604.4

*: obtained by GC after hydrolysis with TFA (4N, 100°C, 4h) for neutral monosaccharides and HCl (6N, 110°C 20h) for glucosamine and insitol residues.

Table II : Molar ratio of ethyl ethers obtained after permethylation of GIPC fractions isolated from *A. fumigatus* mycelium. Molar ratios were calculated by GLC-flame ionisation detection after hydrolysis (TFA, 4N, 6h, 100°C), reduction with $NaBD_4$, and acetylation).

Methyl ethers[a]	Linkages	Glycosphingolipid fractions				
		GSL-U	GSL-A	GSL-B	GSL-C	GSL-D
2,3,4,6-Man	Man-	1.3	1.1	0.1	0.7	-
2,3,5,6-Gal	Gal_f-	-	0.8	0.7	1.1	-
3,4,6-Man	-2-Man-	-	1	1	1	1
2,4,6-Man	-3-Man-	1	1.6	0.7	-	1.1
2,4-Man	-3-^{6}Man-	-	-	-	0.8	-
2,3,5-Gal	-6-Gal_f-	-	-	-	-	+[b]
2,3,4-GlcNAc	-6-GlcN-	0.4	-	-	-	-

[a] : numbers indicate the position of methyl groups
[b] : this methyl ether was observed after hydrolysis by HCl 4N, 4h, 100°C

Table III. ^{1}H and ^{13}C NMR chemical shifts (ppm) and coupling constants ($J_{H,H}$ and $^{1}J_{C1H1}$, Hz) for the glycan sequence of the GSL-U fraction.

α-Manp-(1-3)-α-Manp-(1-6)-α-GlcNH2-(1-2)-Ins-(1-O)-P-Cer

	H_1 $^{3}J_{1,2}$ C_1 $^{1}J_{C1H1}$	H_2 $^{3}J_{2,3}$ C_2	H_3 $^{3}J_{3,4}$ C_3	H_4 $^{3}J_{4,5}$ C_4	H_5 $^{3}J_{5,6}$-$^{3}J_{5,6'}$ C_5	H_6-$H_{6'}$ $^{2}J_{6,6'}$ C_6
α-Man-(1-3)-	4.925 *1.7* 105.26 *169.6*	3.781 *≈3* 73.56	3.606 *≈10* 74.07	3.440 *≈10* 70.57	3.468 *4.9* 76.66	3.524-3.695 *10.9* 64.41
-3)-α-Man-(1-6)-	4.666 *1.8* 103.51 *167.6*	3.932 *3.1* 72.54	3.656 *9.1* 82.24	3.576 9.7 69.06	3.468 *nm -5.0* 76.80	3.518-3.665 *12.00* 64.41
-6)-α-GlcNH2-(1-2)-	5.222 *3.5* 101.32 *nm*	2.923 *10.2* 57.91	3.652 *10.0* 73.83	3.320 *10.8* 72.97	3.994 *≈0 -5.2* 74.30	3.594-3.799 *11.0* 68.29
-2)-*myo*-Ins-(1-O)-P	3.825 *2.7* 79.86 $J_{H,P}$=*10.4*	4.168 *2.7* 85.22	3.278 *10.0* 73.38	3.371 *8.5* 75.18	3.048 $^{3}J_{5,6}$=*8.5* 78.03	3.776 $^{3}J_{6,1}$=*8.8* 75.11

nm : not measured

Table IV. ^{1}H and ^{13}C NMR chemical shifts (ppm) and coupling constants ($J_{H,H}$, $^{1}J_{C1H1}$ and $J_{H,P}$ Hz) for the glycan sequence of the GSL-B fraction.

β-Galf-(1-2)-α-Manp-(1-3)-α-Manp-(1-2)-Ins-(1-O)-P-Cer

	H_1 $^{3}J_{1,2}$ C_1 $^{1}J_{C1H1}$	H_2 $^{3}J_{2,3}$ C_2	H_3 $^{3}J_{3,4}$ C_3	H_4 $^{3}J_{4,5}$ C_4	H_5 $^{3}J_{5,6}$-$^{3}J_{5,6'}$ C_5	H_6-$H_{6'}$ $^{2}J_{6,6'}$ C_6
β-Galf-(1-2)-	4.881 *2.1* 108.70 *173.6*	3.788 *3.2* 83.78	3.808 *5.2* 80.10	3.936 *3.2* 87.25	3.525 *6.7-6.0* 73.90	3.377-3.401 *10.9* 65.85
-2)-α-Man-(1-3)-	5.020 *1.5* 101.71 *169.1*	3.917 *3.8* 77.08	3.607 *8.9* 72.86	3.332 *9.4* 71.05	3.584 *5.0-5.0* 76.30	3.508-3.578 *11.2* 64.00
-3)-α-Man-(1-2)-	5.029 *1.5* 103.85 *173.1*	3.927 *3.3* 72.60	3.659 *9.4* 81.70	3.608 *10.2* 68.81	3.867 *5.8- 3.5* 76.16	3.488-3.561 *11.5* 64.13
-2)-*myo*-Ins-(1-O)-P	3.727 *2.4* 78.99 *139.3* $J_{H1,P}$=*9.2*	3.977 *2.6* 80.91	3.216 *11.3* 73.63	3.351 *8.9* 75.29	2.948 $^{3}J_{5,6}$ *=8.9* 78.56	3.485 $^{3}J_{1,6}$ *=9.4* 75.49

Table V. ^{1}H and ^{13}C NMR chemical shifts (ppm) and coupling constants ($J_{H,H}$ and $^{1}J_{C1H1}$, Hz) for the two glycan sequences of the GSL-A fraction.

GSL-A1: α-Manp-(1-3)-α-Manp-(1-2)-Ins(1-O)-P-Cer

GSL-A2: β-Galf- (1-2)-α-Manp-(1-3)-α-Manp-(1-2)-Ins(1-O)-P-Cer

	H_1 $^{3}J_{1,2}$ C_1 $^{1}J_{C1H1}$	H_2 $^{3}J_{2,3}$ C_2	H_3 $^{3}J_{3,4}$ C_3	H_4 $^{3}J_{4,5}$ C_4	H_5 $^{3}J_{5,6}$-$^{3}J_{5,6'}$ C_5	H_6-$H_{6'}$ C_6
GSL-A1						
α-Manp-(1-3)-	4.905 *2.2* 104.67 *170.0*	3.733 *4.2* 73.47	3.586 *9.4* 74.00	3.446 *8.8* 70.55	3.605 3.595* 76.38 76.42*	3.51-3.58 3.53*-3.60* 64.14 64.05*
-3)-α-Manp-(1-2)-	5.044 *1.7* 103.88 *173.4*	3.932 *4.5* 72.63	3.641 81.5	3.638 *10.2* 68.85	3.889 *6.6* 76.18	3.51-3.58 64.14
-2)-*myo*-Ins-(1-O)-P	3.738 *3.5* 78.94	3.977 *3.4* 80.91	3.227 *9.8* 73.66	3.369 *9.6* 75.24	2.953 *9.6* 78.68	3.501 $^{3}J_{6,1}\approx 9.5$ 75.50
GSL-A2						
β-Galf- (1-2)-	4.901 *1.8* 108.72 *173.8*	3.808 *4.6* 83.79	3.821 *4.0* 80.06	3.956 *4.5* 87.27	3.540 73.90	3.401-3.422 65.84
-2)-α-Manp-(1-3)-	5.035 *1.6* 101.66 *169.2*	3.935 *4.0* 77.09	3.624 *9.4* 72.86	3.364 *9.5* 71.13	3.605 3.595* 76.38 76.42*	3.53-3.60 64.05
-3)-α-Manp-(1-2)-	5.044 *1.7* 103.88 *173.4*	3.951 *4.5* 72.59	3.665 *10.2* 81.85	3.638 *10.2* 68.85	3.889 *6.6* 76.18	3.51-3.58 64.14
-2)-*myo*-Ins-(1-O)-P	3.738 *3.5* 78.94	3.977 *3.4* 80.91	3.227 *9.8* 73.66	3.369 *9.6* 75.24	2.953 *9.6* 78.68	3.501 $^{3}J_{6,1}\approx 9.5$ 75.50

* possible chemical shift

Table VI. ^{1}H and ^{13}C NMR chemical shifts (ppm) and coupling constants ($J_{H,H}$ and $^{1}J_{C1H1}$, Hz) for the two glycan sequences of the GSL-C fraction.

GSL-C1: β-Galf(1-2)-α-Manp(1-3)-[α-Manp (1-6)]-α-Manp-(1-2)- Ins(1-O)-P-Cer

GSL-C2: β-Galf(1-2)-α-Manp(1-3)-[β-Galf (1-6)]-α-Manp-(1-2)- Ins(1-O)-P-Cer

	H_1 $^{3}J_{1,2}$ C_1 $^{1}J_{C1H1}$	H_2 $^{3}J_{2,3}$ C_2	H_3 $^{3}J_{3,4}$ C_3	H_4 $^{3}J_{4,5}$ C_4	H_5 $^{3}J_{5,6}$-$^{3}J_{5,6'}$ C_5	H_6-$H_{6'}$ C_6
GSL-C1						
β-Galf- (1-2)-	4.877 *1.1* 108.47 *174.7*	3.777 *2.9* 83.60	3.800 79.93	3.933 87.07	3.518 73.72	3.360-3.392 65.72
-2)-α-Manp-(1-3)-	4.989 *3.2* 101.72 *169.3*	3.933 *3.5* 76.81	3.604 72.77	3.325 70.79	3.565 76.29	3.507-3.599 3.451*-3.595* 63.74 64.17*
α-Manp-(1-6)-	4.640 *1.5 2.5* 102.57 *169.1*	3.642 *3.1* 73.20	3.506 73.72	3.366 70.07	3.380 76.51	3.445-3.602 64.17
-3,6)-α-Manp-(1-2)-	4.982 *3.2* 103.83 *174.6*	3.924 *2.5* 72.43	3.621 82.02	3.632 68.27	4.021 74.31	3.486-3.702 68.27
-2)-*myo*-Ins-(1-O)-P	3.706 *weak* 78.92	3.949 *4.8* 80.70	3.208 *8.5* 73.43	3.337 *9.0* 75.15	2.936 $^{3}J_{5,6}$= *8.8* 78.49	3.480 $^{3}J_{6,1}$= *9.4* 75.42
GSL-C2						
β-Galf- (1-2)-	4.877 *1.1* 108.47 *174.7*	3.777 *2.9* 83.60	3.800 79.93	3.933 87.07	3.518 73.72	3.360-3.392 65.72
-2)-α-Manp-(1-3)-	5.003 *2.5* 101.63 *169.3*	3.916 *3.4* 76.81	3.594 72.77	3.325 70.79	3.565 76.29	3.507-3.599 3.451*-3.595* 63.74 64.17*
β-Galf-(1-6)-	4.799 *1.9 2.5* 111.1 *171.3*	3.806 *3.7* 84.25	3.779 79.87	3.759 85.71	3.486 73.78	3.507-3.599 3.451*-3.595* 63.74 64.17*
-3,6)-α-Manp-(1-2)-	4.982 *2.6* 103.83 *174.6*	3.921 *2.9* 72.43	3.643 *10.2* 81.58	3.581 *10.2* 68.87	4.013 *6.6* 74.97	3.429-3.747 69.79
-2)-*myo*-Ins-(1-O)-P	3.699 *weak* 78.93	3.967 *4.8* 81.13	3.203 *8.5* 73.43	3.337 *9.0* 75.15	2.936 $^{3}J_{5,6}$= *8.8* 78.49	3.468 $^{3}J_{6,1}$= *9.4* 75.42

* possible chemical shift

Table VII. ^{1}H, ^{13}C and ^{31}P NMR chemical shifts (ppm) and coupling constants ($J_{H,H}$, $^{1}J_{C1H1}$ and $J_{H,P}$, Hz) for the glycan sequence and for the phosphocholine sequence of the GSL-D fraction.

Cho-P-(O-6)-β-Galf-(1-2)-α-Manp-(1-3)-α-Manp-(1-2)-Ins(1-O)-P-Cer

Glycan moiety						
	H_1 $^{3}J_{1,2}$ C_1 P	H_2 $^{3}J_{2,3}$ C_2	H_3 $^{3}J_{3,4}$ C_3	H_4 $^{3}J_{4,5}$ C_4	H_5 $^{3}J_{5,6}$-$^{3}J_{5,6'}$ C_5	H_6-$H_{6'}$ C_6 P
P-(O-6)-β-Galf-(1-2)-	4.939 *1,8* 109.11	3.894 83.74	3.898 79.46	3.974 86.66	3.696 72.11	3.764 68.92 0.763 $J_{H1,P}$=*7.5*
-2)-α-Manp-(1-3)-	5.069 *1.6* 102.24	3.964 *5.2* 77.25	3.672 *9.6* 73.19	3.413 *9.6* 71.07	3.643 76.70	3.651-3.562 64.14
-3)-α-Man-(1-2)-	5.108 *1.9* 103.47	3.959 *4.7* 72.66	3.745 82.26	3.647 68.87	3.958 76.22	3.566 64.29
-2)-*myo*-Ins-(1-O)-P	3.756 *2.4* 79.07 2.974 $J_{H1,P}$=*8.6*	3.982 *2.5* 80.43	3.237 *9.4* 74.07	3.433 *9.1* 75.25	2.973 $^{3}J_{5,6}$ =*9.1* 79.00	3.538 $^{3}J_{1,6}$ =*9.2* 75.74

Choline-phosphate substitution	
	^{1}H ^{13}C ^{31}P
CH_2OP	4.127 61.62 0.763
CH_2N	3.571 68.79
$N(CH_3)_3$	3.169 56.48

Table VIII : GIPC structures described in *Aspergillus fumigatus*

Structures of GIPC	References
α-Man-(1-3)-α-Man-(1-6)-α-GlcN-(1-2)-Ins-P-cer	Toledo *et al.*, 2007; this study
α-Man-(1-3)-α-Man-(1-2)-Ins-P-cer	Levery *et al.*, 2001; Toledo *et al.*, 2007; this study
α-Man-(1-2)-α-Man-(1-3)-α-Man-(1-2)-Ins-P-cer	Toledo *et al.*, 2007
α-Man-(1-3)-[β-Galf-(1-6)]-α-Man-(1-2)-Ins-P-cer	Toledo *et al.*, 2007
α-Man-(1-2)-α-Man-(1-3)-[β-Galf-(1-6)]-α-Man-(1-2)-Ins-P-cer	Toledo *et al.*, 2007
β-Galf-(1-2)-α-Man-(1-3)-α-Man-(1-2)-Ins-P-cer	this study
β-Galf-(1-2)-α-Man-(1-3)-[α-Man-(1-6)]-α-Man-(1-2)-Ins-P-cer	this study
β-Galf-(1-2)-α-Man-(1-3)-[β-Galf-(1-6)]-α-Man-(1-2)-Ins-P-cer	this study
Choline-P-6-β-Galf-(1-2)-α-Man-(1-3)-α-Man-(1-2)-Ins-P-cer	this study